Draft version June 30, 2013
Preprint typeset using LaTeX style emulateapj v. 11/10/09

SPIN-ORBIT MISALIGNMENT FOR THE LONG PERIOD PLANET CANDIDATE KOI-368.01

First Author[1] and Second Author[2]

Draft version June 30, 2013

ABSTRACT

Abstract

Subject headings: keywords

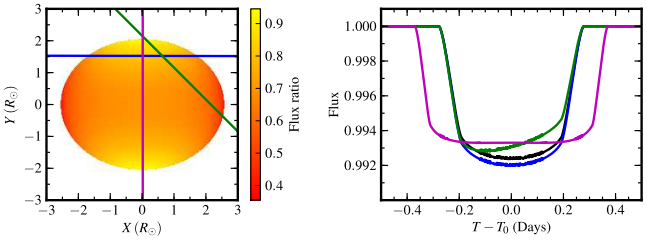

Fig. 1.— f=0.2,beta=1.0,phi=0. Model using koi-368 system parameters (inc, rsum, rratio etc). 0, 45, 90 degree obliquity.

1. INTRODUCTION

2. KOI-368 STELLAR PARAMETERS

[APO observation and spectrum fitting]

The host star rotation period can be identified by searching for spot modulation in the Kepler long cadence PDC lightcurves. We masked out the primary transits and performed a Lomb-Scargle periodogram (Lomb 1976; Scargle 1982) analysis on the lightcurves. A significant peak at 1.19 days was identified, and checked by the CLEAN algorithm (Roberts et al. 1987). [This peak corresponds with vsini and was adopted as the rotation period of the star].

3. ORBIT OBLIQUITY FROM LIGHTCURVE ASYMMETRY

3.1. *Lightcurve model*

3.2. *System parameter fitting*

The transit lightcurve is modelled using the Nelson & Davis (1972) model, implemented in an adaption of the JKTEBOP code (Popper & Etzel 1981; Southworth et al. 2004). The relevant free parameters are orbital period P, transit centre T_0, normalised radius sum $R_\star + R_p/a$, radius ratio $R_p/R_\star$, line of sight inclination i. Quadratic limb darkening coefficients, c_1 and c_2, are fitted for in an initial minimisation routine, with initial estimates taken from Sing (2010), then held fixed for subsequent analyses. Jump parameters for the stellar oblation correction include the planet orbit obliquity λ, stellar oblation f. The projection angle between the stellar rotation axis and line of sight $i_{\rm rot}$ is fixed for an initial analysis, then set free to explore the potential degeneracies. The gravity darkening exponent β is set to be fixed at 0.25 [cite], but also allowed free in subsequent analysis to explore degeneracies. A flux offset for each transit event is calculated and removed at each iteration, and is not included in the fit parameters. For Kepler long cadence data, the model is modified by a 30 minute boxcar smooth. The best fit parameters and the posterior probability distribution is explored via a Markov chain Monte Carlo (MCMC) analysis, using the *emcee* MCMC ensemble sampler (Foreman-Mackey et al. 2012). The likelihood function is given by $\exp(-\Delta\chi^2/2)$. For each transit, we scale the flux errors such that the reduced χ^2 is at unity. This allows for errors other than photon noise to be taken into account.

Figure 2 plots the phase folded transit lightcurve of KOI-368.01 and the best fit spherical and oblate models. The best fit spherical host star model cannot explain the significant in-transit asymmetry observed. The best fit parameters are presented in Table 1.

The posterior probability distributions for relevant parameters are plotted in Figure 3. We find a weak inverse dependency between λ and β, and a positive dependency between λ and $R_p/R_\star$.

3.3. *Asymmetry from eccentricity*

A highly eccentric orbit can also cause asymmetric distortions to the transit lightcurve. An eccentric orbit distorts the lightcurve by changing the planet's velocity through the transit. We explore the possibility that the lightcurve distortions observed for KOI-368.01 are due to an eccentric instead of an oblique orbit.

Following Barnes (2007), we can constrain the change in velocity ($\Delta v = v_{\rm out} - v_{\rm in}$) by measuring the difference in the duration of ingress and egress (Δt),

$$\Delta t = \frac{R_p}{v_{\rm out}\cos\left(\sin^{-1} b\right)} - \frac{R_p}{v_{\rm in}\cos\left(\sin^{-1} b\right)} \quad (1)$$

$$\Delta v \approx v^2 \frac{\Delta t \cos\left(\sin^{-1} b\right)}{R_p} \quad (2)$$

where $b = a\cos i/R_\star = 0.7$ is the transit impact parameter, and $v = \sqrt{GM_\star/a} = 43.3\,{\rm kms}^{-1}$. Using the short cadence data, we measure ingress and egress durations to be equal to within errors of 0.7 minutes, constraining the maximum possible change in velocity to be $\Delta v < 0.5\,{\rm kms}^{-1}$. Figure **??** plots the difference between such an eccentric orbit lightcurve and its best fit circular orbit lightcurve. The maximum in-transit distortions are 10× smaller than that for the oblique orbit model. The maximum distortions during ingress and egress are 5× smaller than that for the oblique orbit model, and are not consistent in shape to that observed for KOI-368.01. The lightcurve distortions for KOI-368.01 therefore cannot be explained by an eccentric orbit.

[1] Affil2; email@email.com
[2] Affil1

TABLE 1
KOI-368 System properties

Parameter	Spherical Model	Limited Oblate Model	Full Oblate Model
Stellar parameters			
$T_{\rm eff}$	9200 ± 500	-	-
$\log g$	4.1 ± 0.5	-	-
[Fe/H]	0.0 ± 0.5	-	-
$v \sin i_{\rm rot}$	100 ± 10	-	-
Lightcurve fitting parameters [1]			
Period (Days)	110.3216229^{+3}_{-7}	110.321615^{+2}_{-6}	110.321613^{+1}_{-7}
T_0 (BJD − 2454000)	1030.36382^{+2}_{-3}	1030.36407^{+6}_{-9}	1030.36440^{+3}_{-1}
$(R_p + R_\star)/a$	0.02101^{+1}_{-3}	0.02078^{+6}_{-5}	0.02103^{+3}_{-2}
$Rp/R_\star$	0.08401^{+4}_{-5}	0.0866^{+1}_{-2}	0.0854^{+1}_{-1}
i	89.209^{+2}_{-1}	89.229^{+3}_{-4}	89.209^{+2}_{-2}
f	-	0.064^{+3}_{-6}	0.038^{+2}_{-2}
λ	-	67^{+6}_{-7}	52^{+5}_{-7}
β	-	-	0.24^{+2}_{-3}
$i_{\rm rot}$	-	-	25^{+4}_{-10}
Derived parameters			

[1] Uncertainties quoted are for the last significant figure

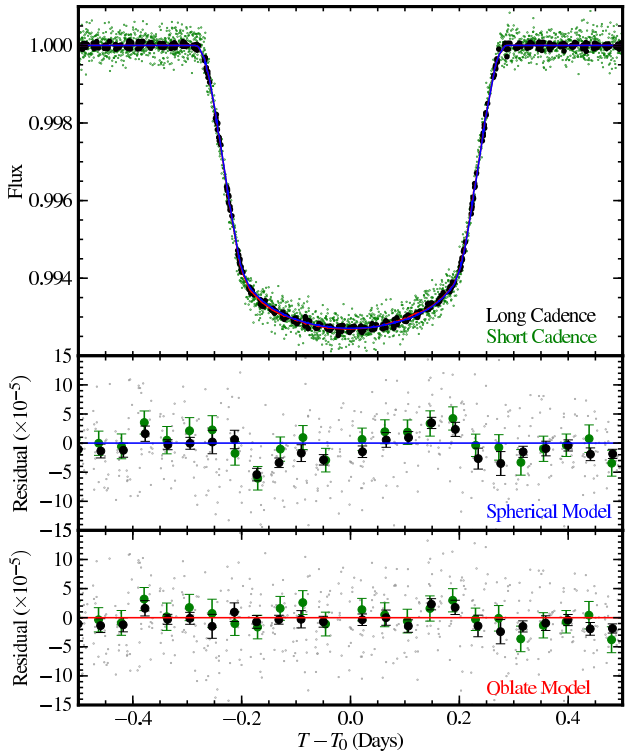

Fig. 2.— Top: Phase folded transit lightcurve of KOI-368.01. Long cadence observations are plotted in black, short cadence in yellow. The best fit transit model for a spherical host star is plotted in blue, oblate host star in red. These two models are indistinguishable at this scale. Middle: Data residual to the spherical host star transit model. The long cadence data are plotted in full as gray dots. Long cadence data binned to 1 hour intervals are plotted in black, binned short cadence residuals in yellow. Bottom: Data residual to the oblate host star transit model.

4. NATURE OF THE COMPANION

[Blends in images]

A stellar mass M-dwarf companion will cause a secondary eclipse in the lightcurve. We mask out the primary transit and remove large scale variations the Kepler long cadence lightcurve using a cosine filter with minimum width of 1 day. We perform a grid search for a secondary eclipse, in the phase space between 0.05 and 0.95, using the Mandel & Agol (2002) eclipse model. We can rule out the presence of any secondary eclipse event with depth $> 10^{-5}$. Assuming the system is not a blend, we can constrain the temperature of the orbiting companion to be < 2500 K, and must be of sub-stellar nature.

4.1. *System eccentricity*

The system eccentricity can be constrained by comparing the measured transit duration ($t_{\rm obs} = 13.2$ hours) against that expected for a circular orbit (e.g. Barnes 2007; Burke 2008; Kane et al. 2012). Adopting host star parameters of $M_\star = 2.2\,M_\odot$ and $R_\star = 2.1\,R_\odot$ [cite/ref], the expected circular orbit transit duration is $t_{\rm circ} = 9.8$ hours. Following Burke (2008), we solve for e in

$$\frac{t_{\rm obs}}{t_{\rm circ}} = \frac{\sqrt{1-e^2}}{1 + e\cos(\omega - \pi/2)}\,, \qquad (3)$$

and find $0.3 < e < 1$, depending on the argument of periastron ω. This range is highly dependent on the assumed host star parameters, which are not well measured. For a host star with 30% smaller radius, we find the eccentricity is constrained to be > 0.9 for all ω. In the case of a host star 30% larger than quoted, we can place no constraints on eccentricity.

5. DISCUSSION

REFERENCES

Barnes, J. W. 2007, PASP, 119, 986

Burke, C. J. 2008, ApJ, 679, 1566

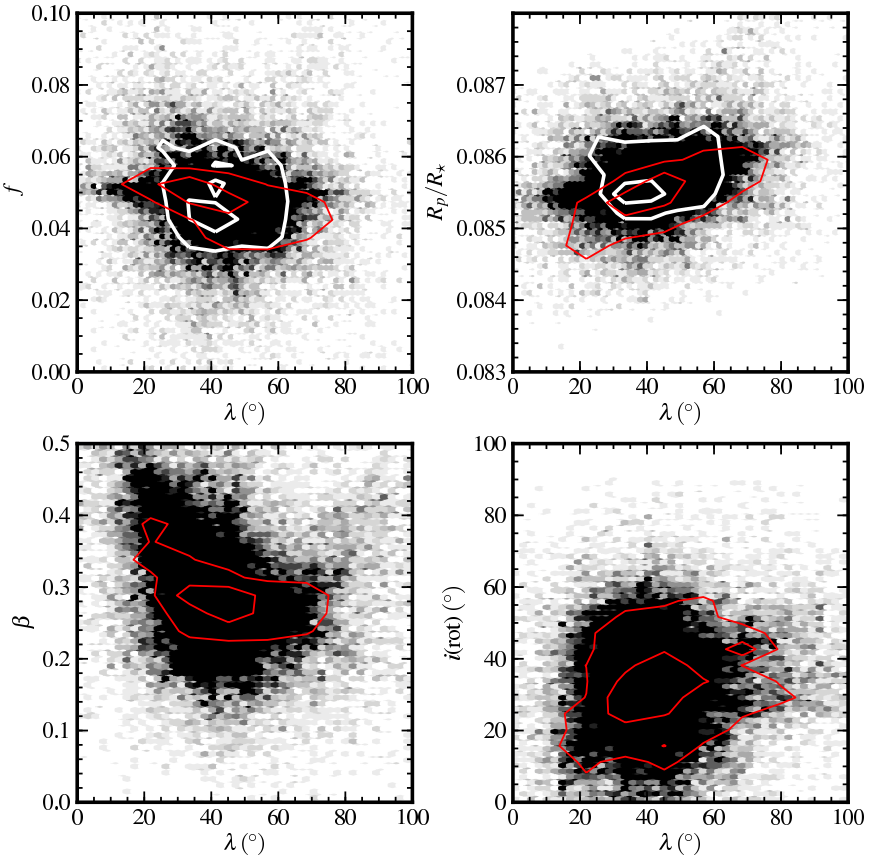

FIG. 3.— Posterior probability distributions showing the correlation between the orbit obliquity λ and stellar oblation f, radius ratio $R_p/R_\star$, gravity darkening exponent β, sky projected angle of the stellar rotation axis $i_{\rm rot}$. The contours mark the 1 and 2σ confidence regions. White contours mark the distribution for the MCMC analysis with β and $i_{\rm rot}$ fixed, the red contours show the distribution with β and $i_{\rm rot}$ set free.

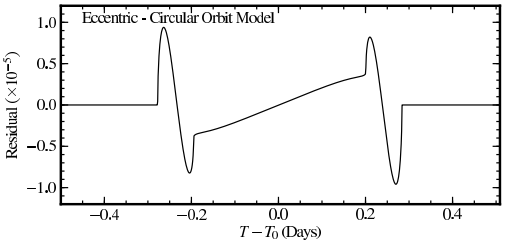

FIG. 4.— The maximum lightcurve distortions due to a eccentric orbit for KOI-368.01 are plotted as residuals to its best fit circular orbit model. The maximum velocity change is determined by measuring the difference in the ingress and egress duration. Eccentricity cannot explain the observe lightcurve asymmetry (Figure 2, middle panel).

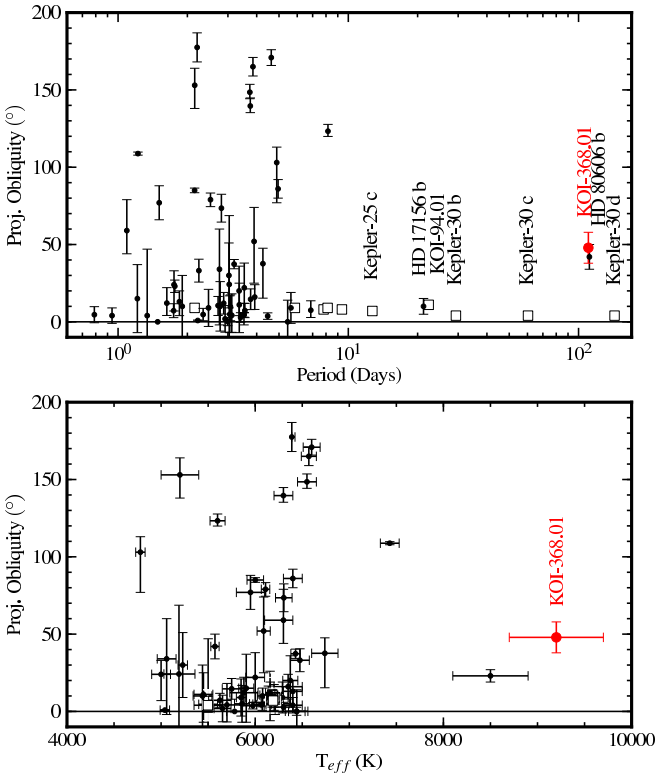

FIG. 5.— caption

Foreman-Mackey, D., Hogg, D. W., Lang, D., & Goodman, J. 2012, ArXiv e-prints

Kane, S. R., Ciardi, D. R., Gelino, D. M., & von Braun, K. 2012, MNRAS, 425, 757

Lomb, N. R. 1976, Ap&SS, 39, 447

Mandel, K., & Agol, E. 2002, ApJ, 580, L171

Nelson, B., & Davis, W. D. 1972, ApJ, 174, 617

Popper, D. M., & Etzel, P. B. 1981, AJ, 86, 102

Roberts, D. H., Lehar, J., & Dreher, J. W. 1987, AJ, 93, 968

Scargle, J. D. 1982, ApJ, 263, 835

Sing, D. K. 2010, A&A, 510, A21

Southworth, J., Maxted, P. F. L., & Smalley, B. 2004, MNRAS, 351, 1277